Dual Fluorescence of Phenyl and Biphenyl Substituted Pyrene Derivatives

Wilfried Weigel* and Wolfgang Rettig

Institute of Chemistry, Humboldt University Berlin, Brook-Taylor-Strasse 2, 12489 Berlin, Germany

Marina Dekhtyar

Institute of Organic Chemistry, Ukrain. Akad. Nauk, Kiew, Ukraine

Claudia Modrakowski, Matthias Beinhoff, and A. Dieter Schlüter

Institute of Organic Chemistry, Free University Berlin, Takustrasse 3, 14195 Berlin, Germany

Received: May 15, 2002; In Final Form: April 1, 2003

The photophysical properties of several acceptor substituted 1-arylpyrene derivatives were investigated. The fluorescence spectra strongly depend on the nature of the aryl moiety and the position and number of methoxycarbonyl acceptor groups. Dual fluorescence, originating from a locally excited and a charge transfer state, was observed for the diester derivatives. The solvent dependence of the dual fluorescence and the slightly curved solvatochromic plots indicate a change of the character of the excited states from solvents of low to high polarity. The rate constants for fluorescence and nonradiative decay were calculated to reveal the nature of the excited-state relaxation, that is, the increase of the mesomeric interactions by geometrical flattening or stabilization of the CT state by further twisting toward perpendicularity. Flattening is the major relaxation pathway of the diester phenylpyrene derivative in nonpolar solvents whereas in highly polar solvents the low value for the fluorescence transition dipole moment (M_f) indicates stabilization of the charge transfer state by further twisting. The fluorescence of the diester biphenylpyrene derivative originates from a locally excited state (LE) in nonpolar solvents. The low value for M_f in polar solvents and the change of the relative intensity of the dual fluorescence signals with the temperature indicate that the red-shifted fluorescence can be assigned to a twisted intramolecular charge transfer state.

Introduction

The solvatochromic effect of the fluorescence of photoexcited molecules that undergo charge transfer (CT) can be applied as a measure to probe the polarity of the surrounding medium. The goal of our long-term project is to quantify a solvent-induced polarity gradient in the interior of dendrimers by exploiting position dependent solvation.[1] Pyrene as the basic chromophore was chosen due to its well documented photophysics and the accessibility of suitable derivatives that would allow incorporation in dendrimer systems.

In general, photoexcited states can undergo stabilization by geometrical relaxation. Especially the conformational changes of systems where the subunits are linked by a single bond have been extensively studied.[2] Flattening in the excited state driven by an increase of mesomeric interactions is one possibility. A prominent example is biphenyl.[3,4]

Some photoexcited donor acceptor systems that undergo CT can reach an energy minimum at the perpendicular conformation characterized by a maximum of the dipole moment.[2,5] For excited systems with partial CT stabilization, both relaxation pathways, planarization or further twisting, can be competitive. Solvent polarity strongly influences the energy of the excited states. This can result in mixing of different states or can lead to multiple fluorescent species, as described for several dimethylaniline derivatives.[5−8] In this context, the fluorescence transition dipole moments are a helpful tool to characterize the nature of the excited states and the relaxation mechanism.[9,10]

One of the well-studied 1-arylpyrenes that undergo excited-state CT is 1-(4-dimethylaminophenyl)pyrene (Py-DMA).[11,12] Pyrene acts as the electron acceptor, whereas the covalently linked aniline subunit constitutes the electron donor. It was found that the emission properties of Py-DMA can be explained by an emitting Franck−Condon state, whereas steric changes such as substitution of *ortho*-hydrogens by methyl groups in the aniline moiety cause an excited-state, large amplitude motion resulting in a strong effect on the spectroscopic and kinetic behavior.

A single emission band with a large Stokes shift was also observed for 4′-(1-pyrenyl)acetophenone in protic solvents.[13] In this case, a broad angular distribution around a shallow excited-state minimum of perpendicular geometry and a flattening of the excited molecule toward a more planar geometry were also considered as rivaling geometrical relaxation pathways. Recently the intramolecular CT properties of 4′-(1-pyrenyl)benzonitrile have been investigated by comparison of transition moments, transient absorption spectra, and INDO/S calculations.[14] These results indicate a relaxation pathway by mutual twisting of the two subunits of this phenylpyrene derivative toward a more planar geometry and exclude the sufficient stabilization of a twisted CT state to become the lowest emitting state. The ultrafast internal conversion of the S_2 state of 4- and 3-(1-pyrenyl)benzoic acid methyl ester leading to the population of the lowest excited state (S_1) that can be described

* To whom correspondence should be addressed. E-mail: weigel@chemie.hu-berlin.de.

10.1021/jp026116u CCC: $25.00
Published on Web 07/11/2003

CHART 1

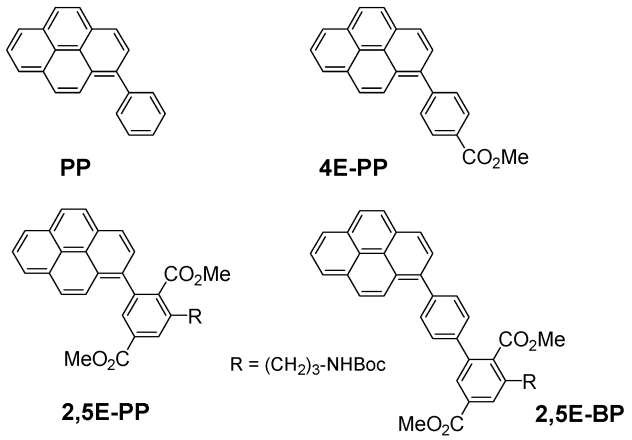

as mixture between locally excited (LE) and CT states was studied by femtosecond pump−probe spectroscopy.[15]

Several isomeric 1-biphenylpyrenes were investigated to address the effect of structural variations on the CT efficiencies in extended donor−acceptor π-systems. It was found that slight changes in the substitution pattern can lead to completely different spectroscopic properties. In addition, the dynamics of the CT strongly change by varying the position of the electron-withdrawing substituent.[16,17]

Dual fluorescence that originates from a locally excited (LE) state and ion pair recombination has been recently reported for pyrene-phenothiazine dyads.[18] In nonpolar solvents, a strong mixing of the ion pair state and the LE state was found.

Here we describe the photophysical properties of four 1-aryl substituted pyrene derivatives with phenyl or biphenyl as the aryl group that vary in the number and position of methoxycarbonyl groups as acceptor at the aryl moiety. The diester derivatives already carry a functional group that will allow incorporation in a dendrimer system. The compounds investigated in this study are shown in Chart 1.

Experimental Part

All 1-arylpyrene derivatives were synthesized via the Suzuki cross-coupling as the key reaction.[19,20] The syntheses are described in detail elsewhere.[1,21] For the fluorescence measurements, the arylpyrene derivatives were purified by preparative HPLC. The purity of the samples was >99.5%.

All solvents used for the spectroscopic measurements were of spectrophotometric grade or have been purified by standard procedures. The solvents used for the solvatochromic measurements (Figure 3) in the order of increasing polarity are methylcyclohexane, dipentyl ether, dibutyl ether, diethyl ether, ethyl acetate, tetrahydrofuran, dichloromethane, butyronitrile, and acetonitrile. UV absorption spectra were measured on an ATI UNICAM series spectrometer UV-4, and the fluorescence spectra were recorded on a SLM AMINCO-Bowman AB 2 spectrofluorimeter. All emission spectra were recorded on a wavelength scale as quanta per nanometer. They are corrected for instrumental sensitivity. For conversion of the spectra to a wavenumber scale and the determination of the fluorescence maxima, the wavelength-dependent intensities were multiplied with λ^2.[22] Deconvolution of superimposed spectra was done by using the log−normal function[23] and least-squares fitting.[24] In the case of 2,5E-BP, the fitting of the dual fluorescence signals was done with locked values for the peak shape and width of the LE band determined from the fitting of the single fluorescence signal in methylcyclohexane. A solution of quinine bisulfate in 0.1 N H_2SO_4 ($\Phi_f = 0.52$) was applied as standard for the measurement of the fluorescence quantum yields.[25] Deoxygenation of the samples was performed by flushing with dry argon.

The fluorescence decay measurements were performed by the principle of time correlated single photon counting (TCSPC)[26] with a conventional setup using an argon ion laser-pumped, passively mode locked Ti:sapphire laser as the excitation source. The pulse duration is about 80 fs, and the repetition rate is 82 MHz. The excitation wavelength was obtained by frequency doubling of the fundamental wavelength of about 700 nm. The fluorescence and scatter were detected by a cooled microchannel plate photomultiplier (MCP, Hamamatsu R 1564 U-01 at −30 °C) coupled to the emission monochromator (Oriel MS257) by means of quartz fiber optics. The signal from a constant fraction discriminator (CFD, Tennelec 454) was used as the start pulse for the time-to-amplitude converter (TAC, Tennelec TC864) operating in the reverse mode. The stop pulses were obtained by imaging a small part of the excitation light on an Antel Si−PIN photodiode (AR-S1). The photodiode and MCP pulses were amplified by homemade microwave amplifiers (INA 10386) and coupled into the CFD. The count rate did not exceed 5 kHz, to avoid pile-up effects. A multichannel analyzer (Fast Comtec MCDLAP) was used for data accumulation. The instrument response function was obtained by detection of Rayleigh scattered light in pure solvents and had a width of 50−60 ps at the excitation wavelength and is dominated by the optical path difference in the monochromator. A detection without the monochromator gave a pulse width of 28 ps. The analysis of the fluorescence decays was done by using Globals Unlimited.[27]

Results and Discussion

Spectroscopic Properties. The normalized absorption and fluorescence spectra of 4E-PP, 2,5E-PP, and 2,5E-BP are shown in Figure 1 along with the spectra of phenylpyrene (PP) as the parent compound. The absorption spectra of all compounds show a single intense band with a maximum around 29 400 cm^{-1} and values of about 4.5 for log ϵ (π,π^* transition). They resemble those of the parent phenylpyrene chromophore. The data for the absorption and fluorescence maxima are summarized in Table 1.

Introduction of a 1-aryl substituent results in a loss of vibrational structure and a stronger tailing in the region above 27 800 cm^{-1}. This indicates some interaction between the π-systems of pyrene and the aryl moiety. The tailing is less pronounced for 2,5E-PP due to the sterical hindrance (twisting) by the *ortho*-ester group. This results in a slightly larger dihedral angle (64°) of the α-single bond, as calculated by AM1 in AMPAC[28,29] in comparison to 57° for 4E-PP. However, it can be assumed that most of the excitation energy is localized on the pyrene moiety.

The lack of a solvatochromic shift of the absorption spectra with increasing solvent polarity is consistent with a small difference between the dipole moments of the Franck−Condon (FC) excited state and the ground state and suggests a small degree of CT in the FC excited state.

Significant differences were found in the fluorescence spectra of the pyrene derivatives with respect to band maxima and solvatochromic effects. In nonpolar solvents such as methylcyclohexane (MCH), the spectra show a maximum between 26 300 and 25 000 cm^{-1} for all compounds, except for 2,5E-PP, which displays a red-shifted fluorescence at 23 000 cm^{-1} (Figure 1). Only the fluorescence spectra of PP show a weak

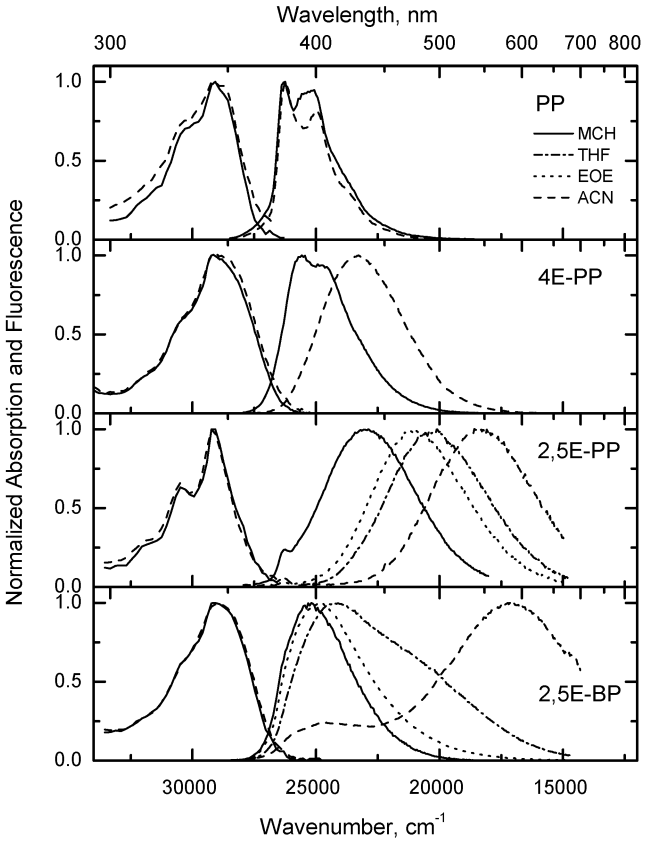

Figure 1. UV absorption and fluorescence spectra in methylcyclohexane (MCH), diethyl ether (EOE), tetrahydrofuran (THF), and acetonitrile (ACN).

TABLE 1: UV Absorption, Fluorescence Maxima, and Stokes Shifts in Methylcyclohexane (MCH) and Acetonitrile (ACN)

	solvent	ν_{abs} (cm^{-1})	ν_f [a,b] (cm^{-1})	$\Delta\nu_{St}$ [c] (cm^{-1})
PP	MCH	29 200	26 300, 25 200	3450[d]
	ACN	29 200	26 200, 25 100	3550[d]
4E-PP	MCH	29 200	25 600, 24 800	4000[d]
	ACN	29 200	23 300	5900
2,5E-PP	MCH	29 200	26 300	2900
			23 000	6200
	ACN	29 100	18 300	10800
2,5E-BP	MCH	29 100	25 200	3900
	ACN	29 100	LE: 24 400	4700
			CT: 17 100	12000

[a] Error less than ±150 cm^{-1}. [b] E_{0-0} = 3.4 eV for PP and 3.3 eV for 4E-PP, 2,5E-PP, and 2,5E-BP in MCH; cf. pyrene with 3.4 eV, ref 39. [c] Error less than 10%. [d] The mean value of the fluorescence maxima is used for calculation of $\Delta\nu_{St}$.

vibrational structure nearly independent of solvent polarity. In comparison, the spectrum of 4E-PP is broader, probably due to some contribution of a CT fluorescence component, and the vibrational structure is completely lost in polar solvents.

The fluorescence maximum of 2,5E-PP in MCH is strongly red-shifted compared to those of all other compounds in the same solvent. This can be explained by a CT that occurs even in nonpolar solvents. The shoulder at 26 300 cm^{-1}, however, indicates that there is still a residual contribution from the LE state. The increase of the LE state versus the CT fluorescence at low temperatures indicates that the CT is connected with a conformational relaxation that can be frozen out by lowering the temperature (Figure 2a).

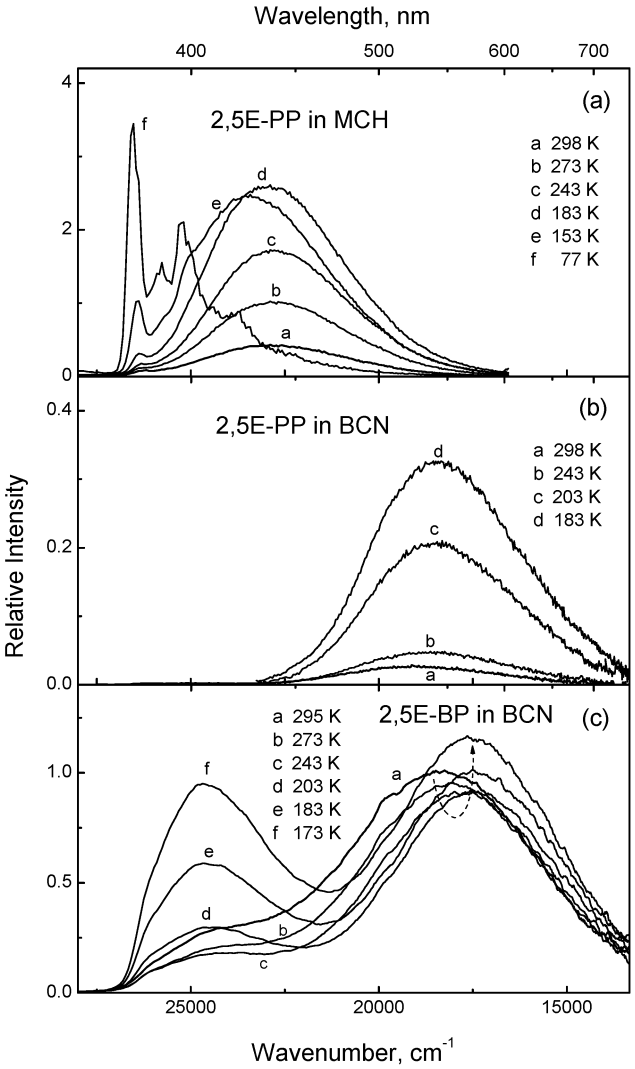

Figure 2. Temperature dependence of the spectral shift and fluorescence intensity of (a) 4E-PP in methylcyclohexane, (b) 2,5E-PP, and (c) 2,5E-BP in butyronitrile.

A pronounced dual fluorescence was observed for the biphenyl derivative 2,5E-BP in solvents of polarity higher than that of tetrahydrofuran with maxima at 24 400 and 17 100 cm^{-1} in acetonitrile (ACN). The spectral distribution is independent of the excitation wavelength. The excitation spectra closely follow the absorption spectra in all solvents. A strong solvatochromic effect was only observed for the red-shifted CT fluorescence band, indicating largely different dipole moments of the two emitting states. As a consequence, the fluorescence bands are assigned to the LE state and a CT state, respectively, with strongly overlapping bands for solvents of intermediate polarity such as diethyl ether and tetrahydrofuran (Figure 1).

Solvatochromic Measurements and Dipole Moments. Solvatochromic measurements were performed in order to investigate the change of the dipole moments between the FC state and the equilibrated S_1 (CT) state. Large red shifts in the order 2,5E-BP > 2,5E-PP > 4E-PP were found by increasing the solvent polarity from MCH to ACN. As expected, the results show a significantly higher CT character for the diester compounds 2,5E-PP and 2,5E-BP. The Stokes shifts ($\Delta\nu_{st}$) calculated from the maxima of the absorption and fluorescence spectra are reported in Table 1. Figure 3 shows a plot of $\Delta\nu_{st}$ versus the macroscopic polarity function $\Delta f = f(\epsilon) - f(n^2)$ that

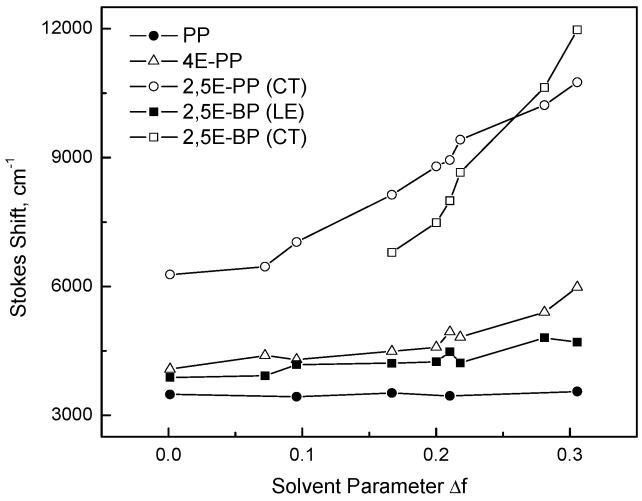

Figure 3. Stokes shifts of the pyrene derivatives in dependence of the solvent parameter Δf. Similar values to those for MCH have been measured in *n*-pentane and cyclopentane.

is calculated from the dielectric constant ϵ and the refractive index n with[30,31]

$$f(\epsilon) = (\epsilon - 1)/(2\epsilon + 1); \quad f(n^2) = (n^2 - 1)/(2n^2 + 1) \qquad (1)$$

In comparison to 4E-PP, the diester derivative 2,5E-PP shows considerably larger values for $\Delta\nu_{st}$. The Stokes shifts of 2,5E-BP were calculated separately for each decomposed band fitted by using the log−normal function[24] in the cases where dual fluorescence was observed.

The dipole moments of the fluorescent state, μ_e^{CT}, can be estimated from the slope m_f of the plot of the energies of the fluorescence maxima versus $\Delta f' = f(\epsilon) - 0.5f(n^2)$ applying eq 2,[32] where a is the solvent cavity (Onsager) radius, calculated from the molecular density formula (eq 3).[33] The states involved in the transition are considered to possess point dipoles located in the center of a spherical cavity. The polarizability of the solute and any specific interaction with the solvent are neglected. The dipole moments of the FC ground state (μ_g^{FC}) are assumed to be identical to μ_g,

$$\nu_f = -[(^1/_4\pi\epsilon_0)(2/hca^3)]\mu_e^{CT}(\mu_e^{CT} - \mu_g^{FC})\Delta f' + \text{constant} \qquad (2)$$

$$a = (3M/4\pi N_a\rho_M)^{1/3} \qquad (3)$$

This approach can only be applied for the solvent range where the dipole moments do not change with Δf. Switching of the character of the fluorescent state by changing the solvent polarity is indicated by the slightly curved plots of 4E-PP and 2,5E-PP and the dual fluorescence of 2,5E-BP. Hence, the values of μ_e of the CT states given as in Table 2 were calculated using m_f determined for the medium- to high-polarity range of the solvents, assuming that in the selected range one excited-state species is dominating. The calculated ground-state dipole moments are seen to be small (<3 D) for all ester derivatives (Table 2). Large values of μ_e^{CT} are obtained for the ester derivatives with an increase from the mono- to the diester compounds. The largest value of μ_e^{CT} is found for the red-shifted band of the dual fluorescence observed for 2,5E-BP. The relatively low value of $\mu_e \approx 9$ D for the high wavenumber emitting state of 2,5E-BP at 25 000 cm^{-1} indicates a small degree of CT (LE character).

TABLE 2: Calculated Ground State and Excited State Dipole Moments Derived from the Slopes (m_f) of the Solvatochromic Plots ν_f versus $\Delta f'$

	μ_g[a] (D)	a[b] (Å)	m_f[c,d] (cm^{-1})	μ_e (D)
PP	0.14	5.5	−300	2.1
4E-PP	2.5	5.8	−11500[e]	13.7
2,5E-PP	2.2	6.9	CT: −15500[e]	21.5
2,5E-BP	1.8	7.2	LE: −2700	9.2
			CT: −39400	37.7

[a] Calculated by AMPAC using AM1; ref 29. [b] Onsager radius calculated by eq 3 with $\rho_M = 1.3$ for PP and 4E-PP and 1.2 g/cm^3 for 2,5E-PP and 2,5E-BP. [c] Error less than 12%. [d] Differences to the slopes calculated from the plot ν_f versus Δf are within the experimental error. [e] Slope from ν_f in all solvents except methylcylohexane and dipentyl ether.

TABLE 3: Fluorescence Quantum Yields, Fluorescence Decay Time, Calculated Rate Constants for Fluorescence and Nonradiative Decay, and Fluorescence Transition Dipole Moments in MCH, Dibutyl Ether (BE), Tetrahydrofuran (THF), Butyronitrile (BCN), and ACN

	solvent	ϕ_f[a]	τ_f[b] (ns)	k_f[c] ($\times 10^7 s^{-1}$)	k_{nr}[c] ($\times 10^7 s^{-1}$)	M_f[d] (D)
PP[e]	MCH	0.4	112	0.36	0.53	0.47
	ACN	0.58	95[f]	0.61	0.44	0.67
4E-PP	MCH	0.49	7.6	6.5	6.7	2.1
	BE	0.56				
	THF	0.83				
	BCN	0.71				
	ACN	0.76	2.7	27.7	8.9	5.4
2,5E-PP	MCH	LE: 0.0005	0.31	0.16	322.4	0.31
		CT: 0.028	1.0	2.8	95.3	1.6
	BE	0.067				
	THF	0.077				
	BCN	0.036				
	ACN	0.0095	2.4	0.39	40.6	0.9
2,5E-BP	MCH	0.50	5.3	9.4	9.5	2.6
	BE	0.41				
	THF	LE: 0.24				
		CT: 0.059				
	BCN	LE: 0.0005				
		CT: 0.0032				
	ACN	LE: 0.0002	0.42	0.29	261	0.87[g]
		CT: 0.0009	0.35			

[a] Error about 10%. [b] Error about 5%. [c] The maximum error for rate constants is about 15%. [d] Error less than 8%. [e] Φ_f and τ_f are determined in deoxygenated solutions; measurement of all other compounds is in aerated solutions. [f] Compare with 109 ns in ACN; ref 12. [g] Calculation of average M_f values from the sum of Φ_f and the average τ_f, using ν_f of CT, consistent with the assumption of an equilibrium between LE and CT states.

Fluorescence Quantum Yield and Lifetime Measurements. The fluorescence quantum yields determined at room temperature in MCH and ACN are reported in Table 3. The Φ_f values for 4E-PP are similar to the values measured for PP. Significantly lower values were measured for the diester derivative 2,5E-PP in nonpolar and polar solvents with the lowest value in ACN. The highest values of Φ_f are observed in solvents of medium polarity. A strong solvent dependence was also found for 2,5E-BP, whereas the overall quantum for the dual fluorescence in ACN is about 2 orders of magnitude lower as compared to the value in MCH. In ACN the relative intensity of the CT band at room temperature is about 5 times higher than the intensity of the LE fluorescence.

Significantly shorter fluorescence decays were measured for all ester derivatives compared to the case of PP. The lifetimes of 4E-PP and 2,5E-BP decrease with increasing solvent polarity, contrary to the case of 2,5E-PP with a lifetime 2 times shorter in MCH than in ACN. A biexponential decay was observed for 2,5E-PP in MCH, where the short-lived component is assigned

to the LE state and the long-lived component to the CT state. Similar lifetime values have been measured for the two bands of the well-resolved dual fluorescence of 2,5E-BP in ACN, indicating an equilibrium of the two excited states.

Nonradiative Decay and Fluorescence Transition Dipole Moments. The fluorescence rate constants ($k_f = \Phi_f/\tau_f$), the corresponding transition dipole moments (M_f, eq 4), and the overall nonradiative deactivation ($k_{nr} = 1/\tau_f - k_f$) were calculated from the fluorescence lifetimes and quantum yields (Table 3). Except for the parent compound PP, a strong solvent dependence of the radiative and nonradiative decay was found. In general, mixing of the low-lying L_b, L_a, and CT states has to be considered for the emission of pyrene derivatives. The contribution of L_a and L_b to the S_1 wave function depends on the relative stabilization of both states by the solvent, which is again dictated by their dipole moments. Mixing of the L_b with the L_a state results in larger M_f values. A compound with very little CT interaction, such as phenylpyrene (PP), for example, shows a fluorescence, similar to that of pyrene, from a low-lying L_b state (forbidden transition) with low k_f and very small M_f values nearly independent of the solvent polarity.

Two geometrical relaxation directions with respect to the single bond connecting the pyrene and aryl moiety are possible after transition to the excited state, flattening of the molecule or further twisting toward a perpendicular geometry. A higher mesomeric interaction of the π-electron system can usually be considered as the driving force for flattening, whereas for the latter case the relaxation to more twisted geometries is governed by the solvent stabilization of the highly polar biradicaloid state. The extreme case of a full charge separated state with an emitting perpendicular average conformation of the donor and acceptor moieties involved is well-known as the TICT (twisted intramolecular charge transfer) state.[2,5−8] The corresponding CT minimum reached by flattening as the main geometrical relaxation pathway of the excited state could be termed as MICT (mesomeric intramolecular charge transfer). In general, MICT states are characterized by strong quinoid contributions and strongly mix with those energetically close lying states which contain a large weight of quinoid resonance structures (e.g. ^1L_a state).

The calculation of the fluorescence transition dipole moments (M_f) and especially of their solvent dependence is a helpful tool to get information about the character of the excited state and the relaxation mechanism (eq 4).[9,10]

$$M_f^2 = (3h/64\pi^4 n^3)(\Phi_f/\tau_f \nu_f^3) \qquad (4)$$

Due to the more planar geometry, a MICT state will be characterized by a higher M_f value (allowed emission) compared to that for a TICT state (forbidden emission). MICT and TICT states can be conformers, that is, potential minima on the same excited-state hypersurface.[2,10] In contrast to the cases of TICT and MICT states, which are delocalized over the complete system, the excitation energy is localized in a typical LE state that is nonpolar or weakly polar and shows little preference upon twisting. The relative energetic stabilization by polar solvents can be expected to be stronger for a TICT state, due to the electronical decoupling of the subsystems by twisting (larger dipole moments).[5] Scheme 1 shows the relative energies of the LE, MICT, and TICT states in dependence of the solvent polarity for the cases of a strong or weak stabilization of the excited CT state by mesomeric interactions. Switching of the character of the lowest excited state (S_1) can be expected by changing the solvent polarity. Scheme 1 also illustrates that, for a certain range of solvent polarities, multiple fluorescence

SCHEME 1: Excited States Stabilized in the Order TICT > MICT ≫ LE with Increasing Solvent Polarity Due to Their Decreasing Dipole Moments in the Same Order[a]

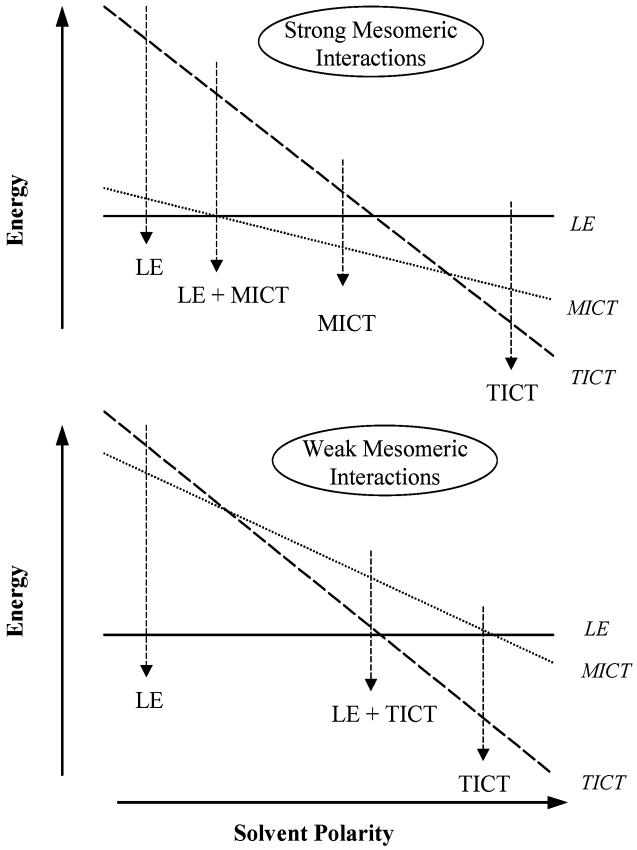

[a] Switching of the character of the lowest excited state (LE, MICT, or TICT) in dependence on the solvent polarity takes place with a different sequence in the case of a strong contribution of mesomeric interactions to the stabilization of the excited state (2,5E-PP) as compared to the case of weak mesomeric interactions (2,5E-BP, higher lying MICT).

with more than two components can occur with changing contributions of the excited states considered.

In comparison to 1-phenylpyrene, 4E-PP is characterized by a higher M_f value for the fluorescence in nonpolar solvents (Table 3). This can be explained by mixing of the forbidden L_b with the more allowed MICT state of L_a/CT character which is lowered in energy due to the presence of the *para*-ester group, introducing partial CT. The higher M_f value observed in polar solvents corresponds to an increased L_a/CT character and is consistent with flattening, that is, MICT formation, of the molecule as the main relaxation pathway.

Nonradiative decay is the major deactivation channel of 2,5E-PP in polar and nonpolar solvents, as indicated by the large k_{nr} values. Correspondingly low Φ_f values are determined. This can probably be explained by the *ortho*-effect of one of the ester groups, which can lead to a new deactivation channel by interaction of the π-obitals of the pyrene system with those of the carbonyl group of one of the ester substituents. A similar effect was reported for 2,3E-PP with a value of 0.008 for Φ_f compared to 0.8 for 3,4E-PP.[34] The significantly lower value of the ^{1}H NMR chemical shifts of the methyl protons for one of the ester groups of 2,5E-PP (3.1 and 3.9 ppm) compared to 2,5E-BP (3.7 and 3.9 ppm)[21] can be explained by an anisotropy effect and is a further indication for a specific interaction due to the proximity of the pyrene system to the *ortho*-ester group.

The red-shifted fluorescence of 2,5E-PP in MCH mainly originates from a low-lying CT state with a high L_a/CT contribution, that is, a large M_f value and MICT character. However, the shoulder at 26300 cm^{-1} indicates dual fluorescence due to a small contribution of LE fluorescence. This is confirmed by the considerable increase of its relative intensity compared to those of the CT fluorescence by lowering the temperature, in contrast to the temperature behavior in highly polar solvents (Figure 2a and b). Due to the low M_f value, the LE emission can be assigned to a low-lying L_b state. The decrease of the M_f value of the CT band by increasing the solvent polarity indicates a decoupling in highly polar solvents such as ACN; the most probable geometrical relaxation coordinate is twisting of the α-bond away from planarity due to two combined effects, the presence of the *ortho*-ester group and the energetic stabilization of the TICT state in ACN.

The *ortho*-ester group of the biphenyl derivative 2,5E-BP is located on the remote phenyl ring. Thus, a special "proximity" decativation channel, as concluded for 2,5E-PP, can be excluded. This is confirmed by the considerably smaller values for k_{nr} in nonpolar solvents. The main contribution of the fluorescence in MCH originates from the LE or MICT state with high L_a/CT character (high M_f value). Increasing the solvent polarity leads to a well visible dual fluorescence with considerable separation of the two bands in highly polar solvents such as ACN. However, the main deactivation pathway is of nonradiative nature, as indicated by the large k_{nr} value and low Φ_f in ACN. Since both of the fluorescent states have similar lifetimes, they can be assumed to be in equilibrium (Scheme 2), and average k_f, M_f, and k_{nr} values were calculated from the overall Φ_f and the average lifetime. The average lifetime has been used, since in the case of a fast equilibrium the observed lifetimes are not the individual decay times of the two excited states but are a weighted average of them.[35] The small value for M_f indicates an increase of the population of highly twisted conformations with increasing solvent polarity.

Figure 2c shows the relative change of the fluorescence intensity of the LE and CT bands in butyronitrile with the temperature. As is typical for a LE−TICT equilibrium,[36] a minimum of the LE intensity relative to the CT fluorescence by lowering the temperature was observed. In addition, a thermochromic red shift of the CT band of 2,5E-BP with decreasing temperature was observed. By comparison with the much smaller effect in the low temperature spectra of 2,5E-PP in butyronitrile (Figure 2b), the red shift can only partially be attributed to the change of the solvent polarity with the temperature, indicating that the relaxation processes on the excited-state surface could be even more complex than discussed.

For an excited-state equilibrium reaction between the LE and CT states, the ratio of the quantum yields Φ_f^{CT}/Φ_f^{LE} is given by eq 5.

$$\Phi_f^{CT}/\Phi_f^{LE} = k_f^{CT}k^{LE\rightarrow CT}/[k_f^{LE}(k^{CT} + k^{LE\leftarrow CT})] \qquad (5)$$

The plot of ln Φ_f versus the inverse temperature is given in Figure 4 and shows a maximum (T_{max} = 260 K) in the ln(Φ_{CT}/Φ_{LE}) curve.

Such a Stevans−Ban plot[37] is typical for a system undergoing a reversible reaction in the excited state, such as an equilibrium between the LE and TICT states.[36] The maximum (T_{max}) of ln(Φ_f^{CT}/Φ_f^{LE}) results from a minimum in Φ_f of the LE fluorescence. Above T_{max} the TICT formation is reversible ($k^{CT} \ll k^{LE\leftarrow CT}$); for temperatures < T_{max} it becomes irreversible ($k^{CT} \gg k^{LE\leftarrow CT}$). The activation energy $E_1^{LE\rightarrow CT}$ was calculated as 8 kJ/mol from the estimated slope ($m = -993$) of the ln(Φ_f^{CT}/Φ_f^{LE}) curve for $T < T_{max}$ according to eq 5 with ($k^{CT} = k_f^{CT} + k_0^{CT}$) and the assumptions that $k^{CT} \gg k^{LE\leftarrow CT}$ and k_f^{CT}/k_f^{LE} and k^{CT} do not depend on temperature. The calculated value of $E_1^{LE\rightarrow CT}$ is close to the value for the activation barrier of the viscosity flow of butyronitrile of 9.3 kJ/mol,[38] indicating that the rate determining step for the formation of the TICT state is governed by viscosity effects.

SCHEME 2: Excited State Dynamic Equilibrium between the Conformatially Different LE and CT Species

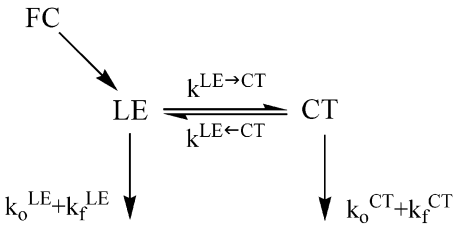

In summary, the nature and the substitution pattern of the 1-aryl substituent of the pyrene derivatives under investigation strongly determine their spectroscopic and kinetic properties. The different tailing of the UV absorption bands reflects the different degrees of interaction of the π-systems of the aryl and pyrene moieties. These compounds undergo substantial CT in the excited state, as indicated by the large solvatochromic shifts of the fluorescence spectra. Well-resolved dual fluorescence was observed for 2,5E-PP in MCH and 2,5E-BP in solvents of medium to high polarity. The change of the relative intensities of the dual fluorescence signals with the solvent polarity indicates a change of the character of the lowest excited states. The dipole moments were calculated for the polarity range of the solvents where the fluorescence can be assumed to originate predominantly from one excited-state species. From the solvent dependence of the k_f and M_f values, conclusions were made regarding changes in the electronic coupling and the relative energy of specific excited states. Flattening (MICT state) is assumed as the geometrical relaxation pathway for 4E-PP independent of the solvent polarity and for 2,5E-PP in solvents of low polarity, in contrast to the cases of 2,5E-PP and 2,5E-BP in highly polar solvents where the low M_f values of the CT fluorescence indicate strong twisting toward perpendicularity on the excited state surface (TICT state). Thus, the emission spectra of 2,5E-PP observed in solvents of medium polarity can be assumed to be a result of the superimposed

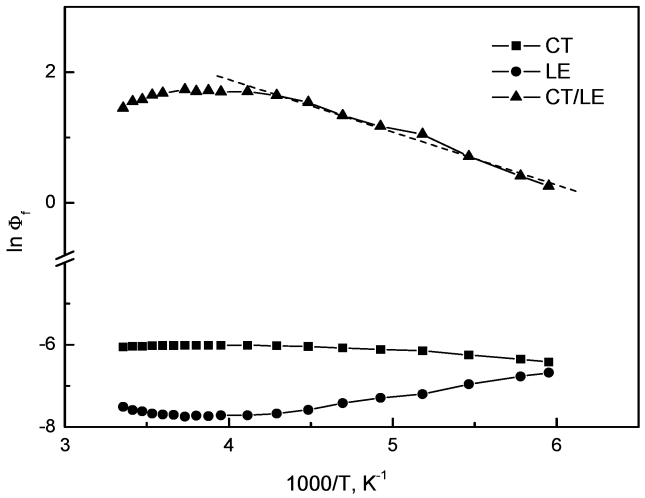

Figure 4. Reciprocal plot of the fluorescence quantum yield vs the temperature of 2,5E-BP in butyronitrile.

fluorescence signals of the MICT and TICT states. The observed dual fluorescence of 2,5E-PP in MCH is assigned to the presence of the nonpolar LE and the polar MICT states. In the case of 2,5E-BP, an excited state equilibrium is assumed to be formed between the LE and the TICT states in highly polar solvents, as revealed by the typical temperature behavior and the similar fluorescence decay times measured for the dual fluorescence.

Acknowledgment. Financial support by the *Deutsche Forschungsgemeinschaft* (DFG within SFB 448) is gratefully acknowledged. We thank Mrs. A. Rothe for valuable help in the spectroscopic measurements.

Supporting Information Available: Examples of the spectral decomposition of the fluorescence spectra of 2,5E-PP in MCH and 2,5E-BP in MCH and THF. This material is available free of charge via the Internet at http://pubs.acs.org.

References and Notes

(1) Beinhoff, M.; Weigel, W.; Jurczok, M.; Rettig, W.; Modrakowski, C.; Brüdgam, I.; Hartl, H.; Schlüter, A. D. *Eur. J. Org. Chem.* **2001**, 3819.

(2) Rettig, W.; Maus, M. Conformational Changes Accompanying Intramolecular Excited-State Electron Transfer. In *Conformational Analysis of Molecules in Excited States*; Waluk, J., Ed.; Wiley: New York, 2000; p 1.

(3) Swiatkowski, G.; Menzel, R.; Rapp, W. *J. Lumin.* **1987**, *37*, 183.

(4) Klock, A.; Rettig, W.; Hofkens, J.; Damme, M. v.; Schryver, F. C. De. *J. Photochem. Photobiol. A: Chem.* **1995**, *85*, 11.

(5) Rettig, W. Photoinduced Charge Separation via Twisted Intramolecular Charge Transfer States. In *Electron-Transfer I*; Mattay, J., Ed.; Springer: Berlin, 1994; Vol. 169; p 253.

(6) Rettig, W. *Angew. Chem., Int. Ed. Engl.* **1986**, *25*, 971.

(7) Grabowski, Z. R.; Rotkiewicz, K.; Siemiarczuk, A.; Cowley, D. J.; Baumann, W. *Nouv. J. Chim.* **1979**, *3*, 443.

(8) Grabowski, Z. R.; Rotkiewicz, K.; Rettig, W. *Chem. Rev.*, submitted.

(9) Maus, M.; Rettig, W.; Depaemelaere, S.; Onkelinx, A.; Schryver, F. C. De.; Iwai, K. *Chem. Phys. Lett.* **1998**, *292*, 115.

(10) Maus, M.; Rettig, W.; Bonafoux, D.; Lapouyade, R. *J. Phys. Chem. A* **1999**, *103*, 2288.

(11) Techert, S.; Schmatz, S.; Wiessner, A.; Staerk, H. *J. Phys. Chem. A* **2000**, *104*, 5700.

(12) Wiessner, A.; Huettman, G.; Kuehnle, W.; Staerk, H. *J. Phys. Chem.* **1995**, *99*, 14923.

(13) Dobkowski, J.; Waluk, J.; Yang, W.; Rulliere, C.; Rettig, W. *New. J. Chem.* **1997**, *21*, 429.

(14) Dobkowski, J.; Rettig, W.; Waluk, J. *Phys. Chem. Chem. Phys.* **2002**, *4*, 4334.

(15) Pandurski, E.; Fiebig, T. *Chem. Phys. Lett.* **2002**, *357*, 272.

(16) Fiebig, T.; Kuehnle, W.; Staerk, H. *Chem. Phys. Lett.* **1998**, *282*, 7.

(17) Fiebig, T.; Stock, K.; Lochbrunner, S.; Riedle, E. *Chem. Phys. Lett.* **2001**, *345*, 81.

(18) Daub, J.; Engl, R.; Kurzawa, J.; Miller, S. E.; Schneider, S.; Stockmann, A.; Wasielewski, M. R. *J. Phys. Chem. A* **2001**, *105*, 5655.

(19) Miyaura, N.; Suzuki, A. *Chem. Rev.* **1995**, *95*, 2457.

(20) Suzuki, A. *J. Organomet. Chem.* **1999**, *576*, 147.

(21) Modrakowski, C.; Flores, S. C.; Beinhoff, M.; Schlüter, A. D. *Synthesis* **2001**, *14*, 2143.

(22) Parker, C. A. *Photoluminescence of Solutions*; Elsevier: Amsterdam, 1968.

(23) Siano, D. B.; Metzler, D. E. *J. Chem. Phys.* **1969**, *51*, 1856.

(24) Using the program: Peakfit, 4.06 ed.; SPSS Inc.: 1995.

(25) Meech, S. R.; Philipps, D. *J. Photochem.* **1983**, *23*, 193.

(26) Connor, D. V.; Philipps, D. *Time Correlated Single Photon Counting*; Academic Press: London, 1984.

(27) Beechen, J. M.; Gratton, E.; Mantulin, O. M. Globals Unlimited, DOS ed.; Laboratory for Fluorescence Dynamics, University of Illinois at Urban-Champaign: Urbana, IL, 1988.

(28) Dewar, M. J. S.; Zoeblich, E. G.; Healy, E. F.; Stewart, J. J. P. *J. Am. Chem. Soc.* **1985**, *107*, 3202.

(29) Dewar, M. J. S.; Stewart, J. J. P.; Quiz, J. M.; Liotard, D.; Healy, E. F.; Deminstan, R. D., II. Ampac 5.0; Semichem: Shawnee, USA, 1994.

(30) Lippert, E. *Z. Naturforsch.* **1955**, *10a*, 541.

(31) Mataga, N.; Kaifu, Y.; Koizumi, M. *Bull. Chem. Soc. Jpn.* **1956**, *29*, 465.

(32) (a) Beens, H.; Knibbe, H.; Weller, A. *J. Phys. Chem.* **1967**, *47*, 1183. (b) Baumann, W.; Bischof, H.; Froehlich, J.-C.; Brittinger, C.; Rettig, W.; Rotkiewicz, K. *J. Photochem. Photobiol., A: Chem.* **1992**, *64*, 49. (c) Il'ichev, Y.; Kuehnle, W.; Zachariasse, K. A. *Chem. Phys.* **1996**, *211*, 441 and references therein.

(33) Roesch, N.; Zerner, M. C. *J. Phys. Chem.* **1994**, *98*, 5817.

(34) Fiebig, T. Ph.D. Thesis, Georg-August-Universität, Göttingen, 1996.

(35) Kapelle, S.; Rettig, W.; Lapouyade, R. *Chem. Phys. Lett.* **2001**, *348*, 416.

(36) Grabowski, Z. R.; Rotkiewicz, K.; Rubaszewska, W.; Kirkor-Kaminska, E. *Acta Phys. Pol.* **1978**, *A54*, 767.

(37) Stevans, B.; Ban, M. I. *Trans. Faraday Soc.* **1964**, *60*, 1515.

(38) Rettig, W. *J. Lumin.* **1980**, *26*, 21.

(39) Berlman, I. B. *Handbook of Fluorescence Spectra of Aromatic Molecules*; Academic Press: New York, 1971.